

Catalytic Growth of N-doped MgO on Mo(001)

Martin Grob,^{1, a)} Marco Pratzer,¹ Marjana Ležaić,² and Markus Morgenstern¹

¹⁾II. Institute of Physics B and JARA-FIT, RWTH Aachen University, D-52074 Aachen, Germany

²⁾Peter-Grünberg Institute, Forschungszentrum Jülich and JARA, D-52425 Jülich, Germany

(Dated: 10 July 2018)

A simple pathway to grow thin films of N-doped MgO (MgO:N), which has been found experimentally to be a ferromagnetic d^0 insulator, is presented. It relies on the catalytic properties of a Mo(001) substrate using growth of Mg in a mixed atmosphere of O_2 and N_2 . Scanning tunneling spectroscopy reveals that the films are insulating and exhibit an N-induced state slightly below the conduction band minimum.

Recently, it has been found that MgO:N-films grown by molecular beam epitaxy (MBE) exhibit ferromagnetism after being annealed at 1020 K.¹ The optimized N-concentration was 2.2 % exhibiting coercive fields as large as 60 mT at $T = 10$ K and magnetic moments per N-atom of $0.3 \mu_B$ barely reducing up to room temperature. A Curie temperature $T_C \simeq 550$ K has been extrapolated and indications that N is incorporated substitutionally on the O-site have been deduced from core level spectroscopy. Moreover, independent studies of N implantation (80 keV) into MgO led to a hysteresis with a coercive field of 30 mT at 300 K.² This raises hope that reliable d^0 ferromagnetism avoiding d-metals can be realized in MgO:N at $T = 300$ K. Such magnetism without d-orbitals has previously been found in thin films of undoped oxides³ including MgO⁴ or defective carbon systems⁵, however, with limited control since relying on defects. ZnO with sp-type dopants as C, N, B, Li, Na, Mg, Al, and Ga shows ferromagnetic signals, too,^{6,7} but, likely, Zn or O vacancies and Zn d-orbitals are involved in the magnetic coupling^{6,8}.

The d^0 ferromagnetism has first been proposed theoretically relying on the double exchange mechanism in narrow impurity bands.⁹ But the high T_C proposed originally has been challenged by going beyond the mean-field approximation¹⁰ or by considering correlation effects,^{11–13}. Partly, even the absence of ferromagnetism was found.¹¹ This renders the high T_C observed experimentally into obvious disagreement to current theory asking for more detailed studies.

MgO:N films, in addition, exhibit bipolar resistive switching behaviour¹⁴ prior to annealing. Resistance contrasts as large as 4 orders of magnitude, switching currents as low as 100 nA and switching times into both states below 10 ns have been obtained.¹ This makes MgO:N also interesting for nonvolatile memories. However, the incorporation of N into MgO is difficult due to the strongly endothermal incorporation of N atoms with respect to N_2 (energy cost per N atom: 10 eV)¹⁵. It requires, e.g., atomic beams of N and O produced by a

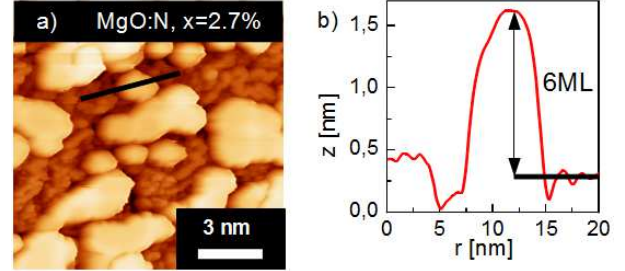


FIG. 1. (Color online) a) STM image of 7 ML $MgO_{0.973}N_{0.027}$ film on Mo(001) with thicker islands (bright areas) on top of a wetting layer of 1-2 ML; $(50 \times 50) \text{ nm}^2$, $U = 3 \text{ V}$, $I = 0.5 \text{ nA}$. b) Line profile along the black line marked in (a) with height of the island above the wetting layer marked.

high-frequency ion plasma source¹ or N^+ implantation². Here, we demonstrate a simplified pathway using the catalytic abilities of a Mo(001) substrate. Thus, we establish a model system of MgO:N for surface science. Mo(001) is chosen since thin MgO films of high quality can be grown epitaxially due to the relatively small lattice mismatch of 6%.^{16–18} Moreover, catalytic properties of Mo with respect to N_2 are known, as, e.g., for the nitrogenase within bacteria using molybdenum enzymes as catalyst.¹⁹ Catalytic N_2 dissociation on surfaces has been induced successfully for the electronically similar W(001), where growth properties of MgO are, however, unknown.^{20–22} We have grown thin films of MgO:N on Mo(001) with thicknesses up to ten monolayer (ML) at optimal doping. Scanning tunneling spectroscopy (STS) revealed that the Fermi level is well within the band gap indicating insulating behaviour of the film. Moreover, an unoccupied state close to the conduction band is found, which is not present in pure MgO films.

The experiments are performed in ultra-high vacuum at a base pressure of $p = 5 \cdot 10^{-11}$ mbar. Firstly, the Mo(100) crystal was cleaned by cyclically annealing within O_2 at initial pressure $p_{O_2} = 5 \cdot 10^{-7}$ mbar and 1400 K, followed by flashing to 2300 K.²³ After every cycle, p_{O_2} is slightly reduced. The MgO:N films are prepared by molecular beam epitaxy of magnesium at $p_{O_2} = 1 \cdot 10^{-7}$ mbar and N_2 pressure $p_{N_2} = 5 \cdot 10^{-6}$ mbar. The deposition temperature T_D is 300 K, if not given explicitly. The depo-

^{a)}corresponding author: grob@physik.rwth-aachen.de

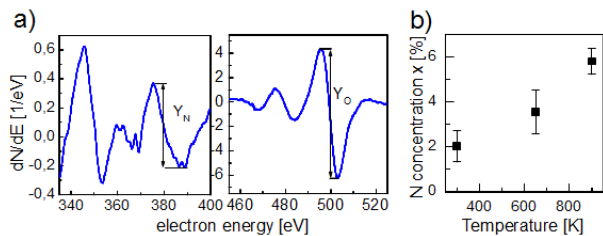


FIG. 2. (Color online) a) Differential AES spectra of N and O for $x = 3.1\%$ with the corresponding peak to peak height Y_i marked. b) Nitrogen concentration x of 7 monolayer thick MgO:N films as a function of deposition temperature T_D .

sition rate of Mg controlled by a quartz micro-balance was 0.5 ML/min. After MgO:N deposition, the samples are annealed at 1100K for 10 min. Figure 1(a) shows a scanning tunneling microscopy (STM) image of 7 ML $\text{MgO}_{0.973}\text{N}_{0.027}$. It exhibits islands on top of an MgO:N wetting layer. From comparison of the coverage determined by the quartz balance and the volume of the MgO:N islands, we estimate the wetting layer thickness to 1-2 ML. We checked crystalline quality and chemical purity of Mo(100) and the MgO:N films by low energy electron diffraction (LEED) and Auger electron spectroscopy (AES). The nitrogen concentration x within the MgO films was determined by AES at primary electron energy of 1 keV being sensitive to the upper 2 nm (9 to 10 ML) only²⁴. The atomic concentration x_i of element i within homogeneous films is calculated from the AES peak height Y_i shown in Fig. 2(a) according to:²⁵

$$x_i = \frac{Y_i/S_i}{\sum_a Y_a/S_a}, \quad (1)$$

where S_i denotes the normalized sensitivity factor and a sums over all relevant elements.

The N concentration x depends on deposition temperature T_D as shown in Fig.2(b) for a 7 ML MgO:N film. Up to $x = 6\%$ is achieved at $T_D = 850\text{K}$ indicating a more effective dissociation of N_2 at higher T_D . Notice that $x = 6\%$ at 7 ML is still far below the amount of N expected from a full N coverage of Mo(001). Next, we prepared MgO:N films with a thickness of up to 100 ML at $T_D = 900\text{K}$. The nitrogen amount within the MgO:N decreased dramatically with film thickness as shown in Fig. 3. A 60 ML thick MgO:N film contained only 0.3% nitrogen in comparison to 3.2% at a thickness of 7 ML. Assuming homogeneous distribution of N, this implies that the amount of N in both films is roughly the same evidencing that N_2 is dissociated on the Mo(100) surface only. We assume that during MgO growth or annealing, the atomic N from the surface is incorporated into the MgO film. To support this scenario, we fit the data assuming a constant areal concentration n of N atoms:

$$x = \frac{n}{d}, \quad (2)$$

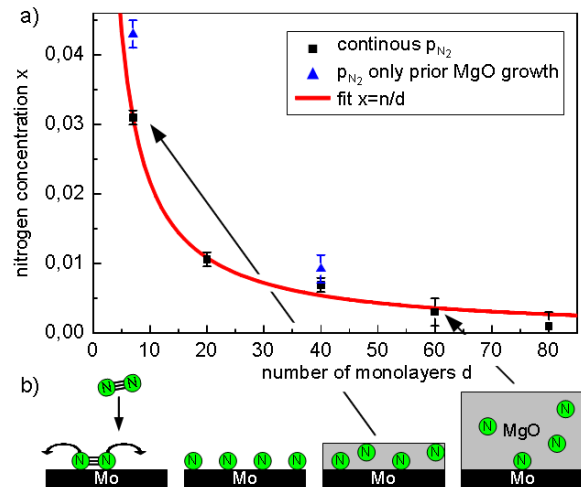


FIG. 3. (Color online) a) Nitrogen concentration x as a function of monolayers d ; different symbols mark different preparation methods; fit curve assumes a constant amount of nitrogen atoms (see text). (b) Sketch of N_2 incorporation: left: N_2 dissociation on Mo(001); right: incorporation of N into MgO leaving the amount of N independent of MgO thickness.

where d denotes the number of MgO ML and n represents the concentration of N atoms with respect to the sum of N and O atoms. If we assume that all N atoms are substitutionally incorporated into the first monolayer of MgO:N, the fit curve plotted in figure 3(a) shows excellent agreement with the measured data points using $n = 21.6\%$. Assuming interstitial impurities, i.e. dumbbells of NO^{15} , equation (2) has to be slightly modified and results in $n = 18.2\%$. Nearly the same n can be achieved by another preparation method: Prior to the deposition of Mg in a pure O_2 environment, we exposed the Mo crystal to N_2 ($p = 5 \cdot 10^{-6}$ mbar) at 300 K for 10 min. Afterwards, we grow MgO without N_2 at $T = 900\text{K}$ leading to very similar N concentrations as shown in Fig. 3(a). Thus, obviously, the dissociation of N_2 takes place at the Mo(001) only. Finally, a third preparation has been performed: 10 ML of pristine MgO were grown first at $p_{\text{N}_2} < 10^{-11}$ mbar. Subsequently, 10 ML MgO:N are deposited at $T_D = 300\text{K}$ and $p_{\text{N}_2} = 5 \cdot 10^{-6}$ mbar. No nitrogen was found in the sample, i.e. $x < 0.2\%$. Thus, if Mo is covered by MgO, the catalytic effect of the substrate is inhibited.

Figure 4 compares STS curves of 11 ML films of $\text{MgO}_{0.96}\text{N}_{0.04}$ and undoped MgO.¹⁸ Doping by N leads to a shift of the Fermi level E_F towards the valence band by about 1 eV and an additional peak with maximum at 0.3 eV below the conduction band minimum (CBM). This is observed for three different N concentrations, i.e. MgO thicknesses, as probed by STS. The peak energy varies laterally by ± 0.3 eV. Density functional (DFT) calculations of bulk MgO with substitutional N predict occupied p-levels close to the valence band maximum (VBM) and an unoccupied, spin polarized level within

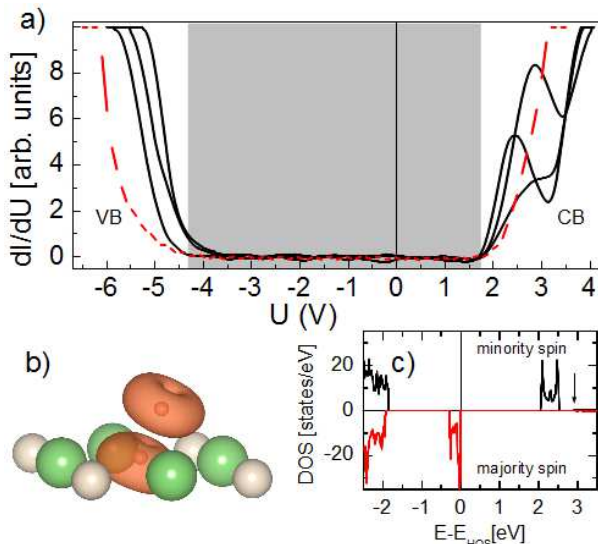


FIG. 4. (Color online) a) $dI/dU(U)$ spectra measured by STS on a 11 ML high $\text{MgO}_{0.96}\text{N}_{0.04}$ island ($U_{\text{stab}} = 3$ V, $I_{\text{stab}} = 0.5$ nA, $U_{\text{mod}} = 40$ mV) at several positions (straight lines) and on a 11 ML thick pristine MgO island (dashed line); average film thickness in both cases: 7 ML. b) Calculated charge density of the unoccupied N-induced states of a N-N dimer at the surface. Large green and small white spheres show Mg and O respectively. c) Calculated density of states (DOS) for N-N dimer at MgO surface, HOS: highest occupied state; all states between -1.2 eV and 3 eV are N-induced; CBM is marked by arrow.

the middle of the band gap, if self interaction correction is included.^{11,12}

This disagrees with our experiment. Since surfaces are not included in these calculations, we performed first-principles DFT calculations including the surface within the spin-polarized generalized gradient approximation²⁶ using projector augmented-wave potentials as implemented in the Vienna Ab initio Simulation Package (VASP).²⁷ Correlation effects on the p-shells of N dopants are accounted for by the DFT+U scheme in Dudarev's approach²⁸ with an on-site effective Coulomb parameter $U_{\text{eff}}=3.4$ eV. A kinetic energy cutoff of 500 eV and a $6 \times 6 \times 1$ Γ -centered k -point mesh was used. The supercell consists of 9 atomic layers MgO(001) using the experimental lattice parameter and a 16 Å thick layer of vacuum. All atomic positions as well as the thickness of the MgO slab were fully relaxed.

Three different configurations with N atoms in the surface layer have been calculated: (i) one N-atom substituting an oxygen, (ii) one N-atom at the interstitial site and (iii) an N-N dimer with one N atom being substitutional and the other at the nearest interstitial site. In case (ii), the calculation was initiated with an N interstitial, but the system relaxed to a configuration where N and O exchanged their places, i.e. N ended up substitutionally and O interstitially. However, the N derived

p-states for case (i) and (ii) are found within 2.2 eV above VBM very similar as for MgO bulk.^{11,12} We conclude that a more complex N structure as, e.g., the N-N dimer at the surface shown in Fig. 4(b) and exhibiting unoccupied N-type p-states close to CBM (Fig. 4(c)), is responsible for the observed peak.

In conclusion, we prepared thin films of N-doped MgO with an N-concentration up to 6% by using the catalytic effect of Mo(001) for N_2 dissociation. Compared with pristine MgO, an additional state close to the conduction band minimum has been observed by STS which could not be attributed to simple N impurity configurations. Helpful discussions with P. Mavropoulos and S. Parkin as well as financial support by SFB 917-A3 and HGF_YIG VH-NG-409 are gratefully acknowledged.

- ¹C. H. Yang, Ph. D. thesis, Stanford university, Stanford 2010.
- ²L. Chun-Ming *et al.*, Chin. Phys. B **20**, 047505 (2011).
- ³M. Ventakesan, C. B. Fitzgerald, and J. M. D. Coey, Nature **430**, 630 (2004); J. M. D. Coey *et al.*, Phys. Rev. B **72**, 024450 (2005); M. Khalid *et al.*, Phys. Rev. B **80**, 035331 (2009); N. H. Hong *et al.*, Phys. Rev. B **73**, 132404 (2006); D. Gao *et al.*, J. Phys. Chem C **114**, 11703 (2010).
- ⁴C. Moyses Araujo *et al.*, Appl. Phys. Lett. **96**, 232505 (2010); C. Martinez-Boubeta *et al.*, Phys. Rev. B **82**, 024405 (2010).
- ⁵P. Esquinazi *et al.*, Phys. Rev. Lett. **91**, 227201 (2003); S. Talapatra *et al.*, Phys. Rev. Lett. **95**, 097201 (2005).
- ⁶H. Pan *et al.*, Phys. Rev. Lett. **99**, 127201 (2007).
- ⁷C. F. Yu *et al.*, J. Phys. D: Appl. Phys **40**, 6497 (2007); S. Chawla *et al.*, Phys. Rev. B **79**, 125204 (2009); J. Appl. Phys. **106**, 113923 (2009) Y. Ma *et al.*, IEEE Trans. Magn. **46**, 1338 (2010).
- ⁸X. L. Li *et al.*, IEEE Trans. Magn. **46**, 1382 (2010); X. G. Xu *et al.*, Appl. Phys. Lett. **97**, 232502 (2010); J. B. Yi *et al.*, Phys. Rev. Lett. **104**, 137201 (2010); D. Gao *et al.*, J. Phys. Chem **14**, 13477 (2010); V. Bhosle and J. Narayan, Appl. Phys. Lett. **93**, 02192 (2008).
- ⁹L.S. Efimov, S. Yunoki, and G. A. Sawatzky, Phys. Rev. Lett. **89**, 216403 (2002); K. Kenmochi *et al.*, Jpn. J. Appl. Phys **43**, L 934 (2004); K. Kenmochi *et al.*, J. Phys. Soc. Jp. **73**, 2952 (2004); V. A. Dinh *et al.*, J. Phys. Soc. Jpn. **75**, 093705 (2006); I. S. Efimov *et al.*, Phys. Rev. Lett. **98**, 137202 (2007).
- ¹⁰P. Mavropoulos, M. Ležaić, and S. Blügel, Phys. Rev. B **80**, 184403 (2009).
- ¹¹A. Droghetti, C.D. Pemmaraju, and S. Sanvito, Phys. Rev. B **78**, 140404 (2008); V. Pardo and W. E. Pickett, Phys. Rev. Lett. **78**, 134427 (2008); H. Wu, A. Stroppa, S. Sakong, S. Picozzi, M. Scheffler, P. Kratzer, Phys. Rev. Lett. **105**, 267203 (2010).
- ¹²I. Slipukhina *et al.*, Phys. Rev. Lett. **107**, 137203 (2011).
- ¹³B. Gu *et al.*, Phys. Rev. B **79**, 024407 (2009).
- ¹⁴R. Waser *et al.*, Adv. Mat. **21**, 2632 (2009).
- ¹⁵M. Pesci *et al.*, J. Phys. Chem. C **1141**, 1350 (2010).
- ¹⁶M.C. Gallagher *et al.*, Thin Solid Films **445**, 90 (2003).
- ¹⁷S. Benedetti *et al.*, Chem. Phys. Lett. **430**, 330 (2006).
- ¹⁸C. Pauly *et al.*, Phys. Rev. B **81**, 125446 (2010).
- ¹⁹J. Chatt *et al.*, Nature **224**, 1201 (1969).
- ²⁰M. Alducin *et al.*, Phys. Rev. Lett. **97**, 056102 (2006).
- ²¹L.R. Clavenna and L.D. Schmidt, Surf. Sci. **22**, 365 (1970).
- ²²C.T. Rettner, E.K. Schweizer, and H. Stein, J. Chem. Phys. **93**, 1442 (1990).
- ²³M. Bode *et al.*, Surf. Sci. **601**, 3308 (2007).
- ²⁴A. Akkerman *et al.*, phys. stat. sol. (b) **198**, 769 (1996).
- ²⁵S. Mroczkowski and D. Lichtmann, J. Vac. Sci. Technol. A **3**, 1860 (1985).
- ²⁶J. P. Perdew *et al.*, Phys. Rev. Lett. **77**, 3865 (1996).
- ²⁷G. Kresse *et al.*, Phys. Rev. B **47**, 558 (1993); **54**, 11169 (1996); **59**, 1758 (1999); P. E. Blöchl, Phys. Rev. B **50**, 17953 (1994).
- ²⁸S. L. Dudarev *et al.*, Phys. Rev. B **57**, 1505 (1998).